Magnetic interference patterns in Josephson junctions with $d+is$ symmetry

N. Stefanakis
Department of Physics, University of Crete, P.O. Box 2208, GR-71003 Heraklion, Crete, Greece and Institute of Electronic Structure and Laser, Foundation for Research and Technology–Hellas, P.O. Box 1527, GR-71110 Heraklion, Crete, Greece

N. Flytzanis
Department of Physics, University of Crete, P.O. Box 2208, GR-71003 Heraklion, Crete, Greece
(Received 13 May 1999; revised manuscript received 9 September 1999)

The magnetic interference pattern and the spontaneous flux in unconventional Josephson junctions of superconductors with $d+is$ symmetry are calculated for different reduced junction lengths and the relative factor of the *d*- and *s*-wave components. This is a time-reversal broken symmetry state. We study the stability of the fractional vortex and antivortex which are spontaneously formed and examine their evolution as we change the length and the relative factor of *d*- and *s*-wave components. Asymmetry in the field-modulated diffraction pattern exists for lengths as long as $L=10\lambda_J$.

I. INTRODUCTION

In the past several years one of the main questions in the research activity on high-T_c superconductors has been the identification of the order parameter symmetry.[1–5] The most possible scenario is that the pairing state is an admixture of a dominant *d* wave with some small *s*-wave component. This fact is a direct consequence of the orthorhombic distortion of the systems which makes both the *d* wave and *s* wave indistinguishable (they transform according to the identity representation of the group). There is a basic difference in the physics if one takes into account the phase difference between the two parts of the order parameter. The mixing due to orthorhombicity predicts a $d+s$ or equivalently $d-s$ order parameter. This has been analyzed within the Ginzburg-Landau framework, valid close to T_c.[6] Experimental observation of this possibility has been clearly realized in photoemission experiments[7] and the *c*-axis tunneling.[8]

In addition to the above work, calculations based in BCS weak-coupling theory[9,10] predict that a mixed symmetry is realized in a certain range of interaction. This state has the time-reversal symmetry $\mathcal{T}$ broken. This symmetry $(d+is)$ is realized in bulk calculations only as a consequence of the absence of any orthorhombic distortion (the Fermi surface is either circular or tetragonal in the particular examples) which favors a phase difference of $\pi/2$ between the two components as opposed to π in the presence of it.

The situation becomes more complicated if we consider surface effects. The observation of fractional vortices on the grain boundary in $YBa_2Cu_3O_7$ by Kirtley *et al.*[11] may indicate a possible violation of the time-reversal symmetry near grain boundary (because the boundary breaks the bulk orthorhombic symmetry). Therefore it is interesting to study more this symmetry in the case of interfaces.

In the present paper we study the static properties of a one-dimensional junction which contains a twin boundary where the pair transfer integral between the two superconductors has an extra relative phase in each twin. The maximum current I_c that a junction can carry versus the external magnetic field H in the direction parallel to the plane of the junction is calculated by solving numerically the sine-Gordon equation. The stability of fractional vortices f_v or antivortices f_{av}, which are spontaneously formed as a consequence of the symmetry, is examined in the absence of current and magnetic field for different lengths and relative phases.

In the $\mathcal{T}$-violated state the magnetic interference pattern as has been obtained by Zhu *et al.*[12] in the short-junction limit is asymmetric. They conclude that for a long junction the magnetically modulated critical current is basically identical to the conventional 0-0 junction due to the formation of the spontaneous vortex near the center of the junction. Our exact numerical calculations show that there is a ''dip'' near the center of the diffraction patterns even for junctions as long as $10\lambda_J$.

The rest of the paper is organized as follows. In Sec. II we discuss the Josephson effect between two superconductors with mixed *s*- and *d*-wave symmetry. In Sec. III the role of the twin boundary is discussed. In Sec. IV we present the results for the magnetic flux and the interference pattern. Finally, a summary and discussion are presented in the last section.

II. JOSEPHSON EFFECT BETWEEN TWO SUPERCONDUCTORS WITH MIXED WAVE SYMMETRY

We consider two superconductors (A and B), with a two-component order parameter $(n_1^{A(B)}, n_2^{A(B)})$, which are separated by an intermediate layer of thickness t in the z direction, as seen in Fig. 1(a). If the angles between the crystalline a axis of each superconductor A and B with the junction interface are defined as θ_1 and θ_2, respectively, the bulk order parameters n_1 for the *d*-wave component and n_2 for the *s*-wave component, near the interface can be written as

$$n_1=\begin{cases}\tilde{n}_1^A e^{i\phi_1^A}=n_{10}\cos(2\theta_1)e^{i\phi_1^A}, & z>t,\\ \tilde{n}_1^B e^{i\phi_1^B}=n_{10}\cos(2\theta_2)e^{i\phi_1^B}, & z<0,\end{cases} \tag{1}$$

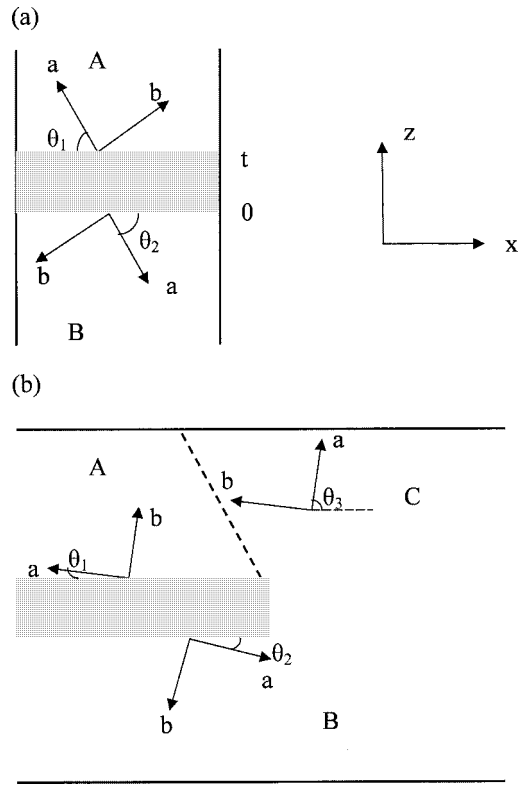

FIG. 1. (a) A single Josephson junction between superconductors A and B with a two-component order parameter. The angle between the crystalline a axis of A (B) and the junction interface is θ_1 (θ_2). (b) The geometry of the junction between the twinned crystal (regions A and C) and the untwinned crystal B. The dashed line marks the twin boundary.

and

$$n_2=\begin{cases}\tilde{n}_2^A e^{i\phi_2^A}=n_{20}e^{i\phi_2^A}, & z>t,\\ \tilde{n}_2^B e^{i\phi_2^B}=n_{20}e^{i\phi_2^B}, & z<0.\end{cases} \tag{2}$$

Here ϕ_1^μ and ϕ_2^μ, $\mu=A,B$, are the phases of the order parameters in superconductors A and B.

The expression for the supercurrent density can be obtained by the Ginzburg-Landau equations[12,13] as a function of the two order parameters and evaluated at the interface to find the tunneling current density. For this we need the solution of the order parameter in the interface which is obtained by using the approximation of small thickness compared to the coherence length,[14] with boundary conditions as given by Eqs. (1) and (2). The approximation leads to a linear variation of the order parameter across the interface. Then the supercurrent density can be written as

$$J=\sum_{i,j=1}^{2} J_{cij}\sin(\phi_i^B-\phi_j^A), \tag{3}$$

where

$$J_{c11}=(2e/m_d^* t)\tilde{n}_1^A\tilde{n}_1^B,$$

$$J_{c21}=(2e/m_\nu^* t)\tilde{n}_1^A\tilde{n}_2^B,$$

$$J_{c12}=(2e/m_\nu^* t)\tilde{n}_2^A\tilde{n}_1^B,$$

$$J_{c22}=(2e/m_s^* t)\tilde{n}_2^A\tilde{n}_2^B \tag{4}$$

are implicit functions of the orientation of the crystalline axis through the tilded order parameters as seen in Eqs. (1) and (2); m_d, m_ν, m_s are the effective masses that enter into the Ginzburg-Landau equations.

Some special cases are the following.

(i) For d-wave symmetry one component of the order parameter vanishes at the interface ($n_2=0$). The Josephson current density becomes $J=|J_{c11}|\sin(\phi+\phi_c)$ with $\phi_c=0$ for $J_{c11}>0$ and $\phi_c=\pi$ for $J_{c11}<0$.

(ii) For $(d+s)$ wave and the restriction where $\phi_2^A-\phi_1^A=\phi_2^B-\phi_1^B=\pi$ is fixed on both sides of the interface, the current density J depends only on one phase difference through the interface, say, $\phi=\phi_1^B-\phi_1^A$, and

$$J(\phi)=|\tilde{J}_c|\sin(\phi+\phi_c), \tag{5}$$

with

$$\tilde{J}_c=J_{c11}+J_{c22}-J_{c12}-J_{c21}. \tag{6}$$

In Eq. (5), $\phi_c=0$ for $\tilde{J}_c>0$ and $\phi_c=\pi$ for $\tilde{J}_c<0$.

(iii) For the $(d+is)$-wave case the intrinsic phase difference within each superconductor A and B can be assumed to be $\phi_2^A-\phi_1^A=\phi_2^B-\phi_1^B=\pi/2$. The current density J is

$$J(\phi)=\tilde{J}_c\sin(\phi+\phi_c), \tag{7}$$

with

$$\tilde{J}_c=\sqrt{(J_{c11}+J_{c22})^2+(J_{c12}-J_{c21})^2}, \tag{8}$$

$$\phi_c=\begin{cases}\tan^{-1}\dfrac{J_2}{J_1}, & J_1>0,\\ \pi+\tan^{-1}\dfrac{J_2}{J_1}, & J_1<0,\end{cases} \tag{9}$$

where $J_1=J_{c11}+J_{c22}$, $J_2=J_{c21}-J_{c12}$. Equation (9), through Eqs. (1), (2), and (4), defines the relationship between θ_1, θ_2 and the phase ϕ_c.

III. ROLE OF THE TWIN BOUNDARY

We consider two superconducting sheets A and C which overlap for a distance L with the superconducting sheet B, in the x direction, [as shown in Fig. 1(b)]. The relative phase of the s- and d-wave order parameters in all three superconducting regions is assumed to be $\pi/2$. The regions A and C are separated with a twin boundary, with odd reflection symmetry. At an odd reflection symmetry twin boundary, the relative orientation of the a and b axes changes by $\pi/2$ on reflection across the twin boundary, and the lobes of the s and d order parameters with different sign face each other along the boundary.[15] This symmetry is a consequence of the dominant d-wave order parameter that we have assumed, and the fact that the order parameter is continuous and varies as little as possible at the twin boundary. Experiments have shown that the transition temperature (T_c) of a twinned crystal remains the same following the removal of the twin

boundary.[16] We then choose the angle between the a axis in region A and the x direction to be $\theta_1 = 15°$, causing the angle between the a axis and the junction interface in region C to be $\theta_3 = 75°$. The missorientation angle of superconductor B with the junction interface is $\theta_2 = 22.5°$. This choice of angles was made intentionally in order to compare our results with those of Ref. 12. With the above arrangement a simple calculation from Eq. (9) yields $\phi_{c1} = 0.01\pi$ in $0 < x < L/2$ and $\phi_{c2} = 1.08\pi$ in $L/2 < x < L$. The current transport across the junction is taken to be only along the z direction. We describe the entire junction with width w small compared to λ_J in the y direction, of length L in the x direction, and in external magnetic field H in the y direction. We expect that experiments in Josephson junctions between twinned and untwinned superconductors will show the results that we present. Our analysis can equally well apply to explain the results of Ref. 11. The superconducting phase difference ϕ across the junction is then the solution of the sine-Gordon equation

$$\frac{d^2\phi(x)}{dx^2} = \frac{1}{\lambda_J^2}\sin[\phi(x) + \phi_c(x)], \tag{10}$$

with the inline boundary conditions

$$\left.\frac{d\phi}{dx}\right|_{x=0,L} = \pm\frac{I}{2} + H. \tag{11}$$

The Josephson penetration depth is given by

$$\lambda_J = \sqrt{\frac{\hbar c^2}{8\pi e d \tilde{J}_c}},$$

where d is the sum of the penetration depths in two superconductors plus the thickness of the insulator layer. We also assume that the critical current density $\tilde{J}_c$ is constant within each segment of the interface.

The spatial variation of ϕ induces a local magnetic field given by the expression

$$\mathcal{H}(x) = \frac{\Phi_0}{2\pi t}\frac{d\phi(x)}{dx}. \tag{12}$$

We can classify the different solutions obtained from Eq. (10) with their magnetic flux content

$$\Phi = \frac{\Phi_0}{2\pi}(\phi_R - \phi_L), \tag{13}$$

where $\phi_{R(L)}$ is the value of ϕ at the right(left) edge of the junction, and $\Phi_0 = hc/2e$ is the flux quantum.

To check the stability we consider small perturbations $u(x,t) = v(x)e^{st}$ on the static solution $\phi(x)$, and linearize the time-dependent sine-Gordon equation to obtain

$$\frac{d^2v(x)}{dx^2} + \cos[\phi(x) + \phi_c(x)]v(x) = \lambda v(x), \tag{14}$$

under the boundary conditions $dv(x)/dx|_{x=0,L} = 0$, where $\lambda = -s^2$. It is seen that if the eigenvalue equation has a negative eigenvalue the static solution $\phi(x)$ is unstable.

We can also compute the free energy of the solution for zero current and external magnetic field:

$$F = \frac{\hbar \tilde{J}_c w}{2e}\int_0^L \left[1 - \cos[\phi(x) + \phi_c(x)] + \frac{\lambda_J^2}{2}\left(\frac{\partial\phi}{\partial x}\right)^2\right]dx. \tag{15}$$

Note that the no-vortex solution $\phi = 0$ everywhere is not a solution of this problem.

When $\phi_{c1} = \phi_{c2} = 0$ we have the conventional s-wave junction. In case $\phi_{c1} = 0$, $\phi_{c2} = \pi$ we have the d-wave or $(d+s)$-wave junction. The above cases have time-reversal symmetry ($\mathcal{T}$ conservation). When ϕ_{c1}, ϕ_{c2} are slightly different from 0 and π, we have the $(d+is)$-wave pairing, which is a broken time-reversal symmetry state ($\mathcal{T}$ violation). In this work, the particular parameters we use are $\phi_{c1} = 0.01\pi$, $\phi_{c2} = 1.08\pi$, and the pairing state is $(d+is)$.

IV. SPONTANEOUS MAGNETIC FLUX AND INTERFERENCE PATTERNS FOR THE $\mathcal{T}$-VIOLATING PAIRING STATE

We consider first a symmetric 0-π junction. Here the change of ϕ_c from 0 to π introduces spontaneous flux lines, i.e., vortices with half the conventional flux quantum ($\Phi = \pm\Phi_0/2$), if the junction length is much larger then λ_J. We call them half-vortex (h_v) and antivortex (h_{av}) solutions. To obtain these vortices as solutions of Eq. (10) for zero current and magnetic field, a kink or antikink like initial condition is used, which is iterated until convergence. Using the h_v and h_{av} solutions as initial conditions and increasing the current we are able to reach the critical current I_c for a given magnetic field. In Fig. 2 we plot the critical current I_c as a function of the magnetic flux Φ (in units of Φ_0) for different junction lengths: (a) $L = 10$, (b) $L = 4$, (c) $L = 2$, and (d) $L = 1$ ($\lambda_J = 1$). The circles (squares) in this figure correspond to the half vortex (antivortex) branch. For most of the range of existence of h_v (h_{av}) the magnetic flux is positive (negative) while there is a small region where it turns into an antivortex (vortex). A similar calculation has been done in Refs. 17 and 18 where they considered only the h_v solution. As we can see, there is a ''dip'' at $\Phi = 0$, for lengths as long as $L = 10$.

In the $(d+is)$-wave case, where $\phi_{c1} = 0.01\pi$ and $\phi_{c2} = 1.08\pi$, the phase ϕ must form a kink or antikink near $x = 0$ in order to match the conditions on both sides. A new flux quantization appears $\Phi = \chi\Phi_0$ where χ is neither integer nor half-integer. We call the solution with positive flux a fractional vortex (f_v) while the negative-flux solution is the fractional antivortex (f_{av}). Note that χ is equal to $1 - (\phi_{c2} - \phi_{c1})/2\pi$ for the (f_v) solution[12] and $(-\phi_{c2} + \phi_{c1})/2\pi$ for the (f_{av}) in the long-junction limit. In Fig. 3 we present our calculations for the $\mathcal{T}$-violation case where $\phi_{c1} = 0.01\pi$ and $\phi_{c2} = 1.08\pi$. We also plot for $L = 1$ the analytical result (solid line) of Zhu *et al.*[12] In contrast to the pure d-wave case, for small lengths this pattern is asymmetric and the ''dip'' in the maximum current does not occur at $\Phi = 0$, but at a finite Φ value. This behavior also exists for lengths as long as $L = 10$.

If we plot I_c vs H (and not Φ), then the two branches in Fig. 3 will be almost coincident and one might draw the

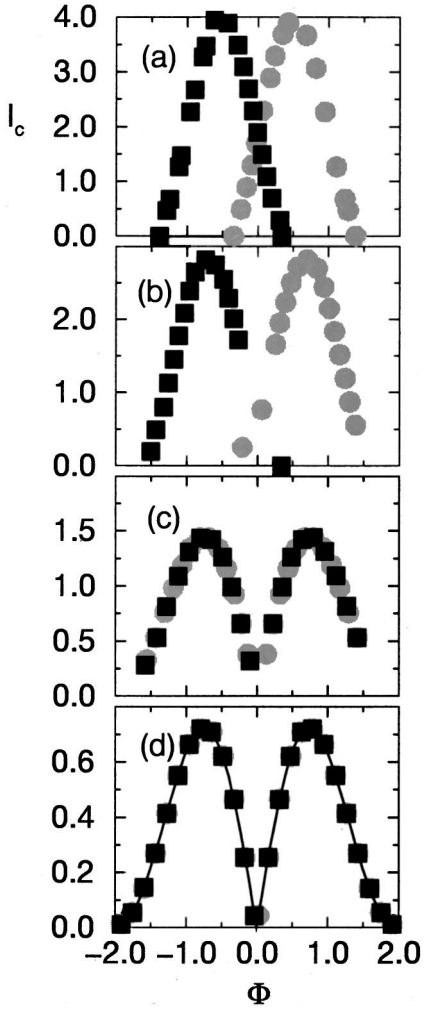

FIG. 2. Critical current I_c versus the magnetic flux Φ (in units of Φ_0) for a symmetric 0-π junction, for different junction lengths: (a) $L=10$, (b) $L=4$, (c) $L=2$, and (d) $L=1$.

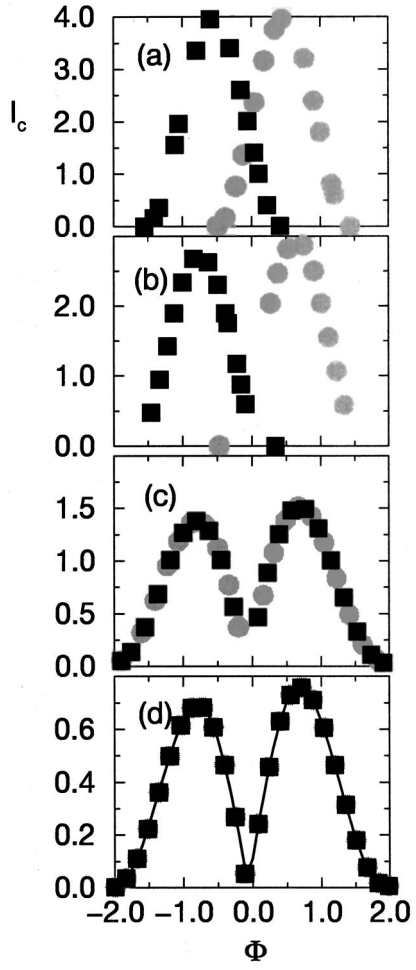

FIG. 3. Critical current I_c versus the magnetic flux Φ for a junction with $d+is$ symmetry, $\phi_{c1}=0.01\pi$, $\phi_{c2}=1.08\pi$, for different junction lengths: (a) $L=10$, (b) $L=4$, (c) $L=2$, and (d) $L=1$.

conclusion that the behavior for a long junction is the same independent of the symmetry. The proper quantity to consider though is the total magnetic flux which includes both the contribution from the external field and the induced self-field. It should be remarked that for an *s*-wave junction the relation between Φ and H is linear for small H so that the plot of I_c vs H or Φ does not show any differences for small H. For higher H, however, the overlapping branches (for long L) are unfolded. In the case of a different symmetry even the small H form can change due to the existence of spontaneous magnetization.

In Figs. 3(a) and 3(b) both f_v and f_{av} branches are stable. There are also unstable branches which are not presented, but are seen in Fig. 3(c). The I_c almost coincides for two solutions, one of which is stable and the other unstable. Still we can distinguish the two peaks corresponding to f_v and f_{av}. As expected for the short length ($L=1$) the stable and unstable branches are exactly coincident. These unstable branches also exist for longer lengths but we need different initial conditions to obtain them due to the strong nonlinear dependence of Φ on the magnetic field H. In the calculations we vary nonmonotonically the magnetic field, but the slope of $\Phi(H)$ changes sign near the boundary separating the stable and unstable solution.

Figure 4 addresses the question of spontaneous flux generation in junctions with broken time-reversal symmetry ($\mathcal{T}$ violation) as a function of the reduced length (L) and the relative factor of *s* and *d* components. The long-dashed line is the result of Ref. 12 which compares with our numerical result (solid line). Both cases have $\phi_{c1}=0.01\pi$, $\phi_{c2}=1.08\pi$. The approximation they made is that the formation of the spontaneous vortex at the junction center simply changes the phase in the left (right) part of the junction by ϕ_{c1} (ϕ_{c2}). This approximation is valid for long junctions but as we can see in Fig. 4 does not hold for junctions with lengths less than $10\lambda_J$, since the exponentially decaying analytic solution does not satisfy the zero-current boundary conditions at the ends. We have also used two other values for ϕ_{c2}, i.e., 0.9π (dotted line) and 0.8π (dashed line). We conclude that as we decrease the value of ϕ_{c2} the fractional vortex f_v tends out to be a 2π vortex, whereas the fractional antivortex gradually loses its flux content.

In Fig. 5(a) we have plotted the magnetic flux Φ (solid line, $\Phi_0=1$) versus the value ϕ_{c2} for $L=10$ and $H=0$. In the limit $\phi_{c2}=0$ and $\phi_{c1}=0$ the junction behaves as the usual *s*-type junction,[19] where the different solutions are distinguished by the number of complete vortices present in the junction. Solutions where the junction contains more than n

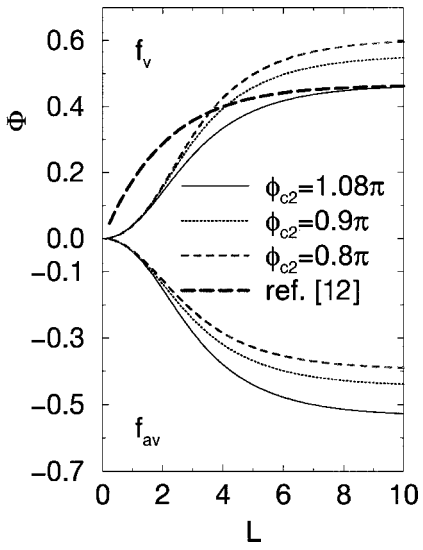

FIG. 4. The spontaneous magnetic flux Φ as a function of the reduced junction length L, for different values of the intrinsic phase ϕ_{c2} in the right part $L/2<x<L$ of the junction and $\phi_{c1}=0.01\pi$.

and fewer than $n+1$ vortices we say that they belong to the $(n, n+1)$ branch. In this case the only stable solution present in the junction is that with $\phi=0$ everywhere. This solution has magnetic flux $\Phi=0$ and belongs to the (0,1) branch. The vortex and antivortex solutions with $\Phi=1$ and $\Phi=-1$, respectively, also exists for $H=0$, but as seen in Ref. 20 are unstable. As we increase the value ϕ_{c2}, the no-vortex solution with $\Phi=0$ of the usual *s*-type junction is transformed to the fractional antivortex f_{av}. If we further increase ϕ_{c2} (not presented in the figure), it will reach the full antivortex of the *s*-wave junction when $\phi_{c2}=2\pi$. Be-

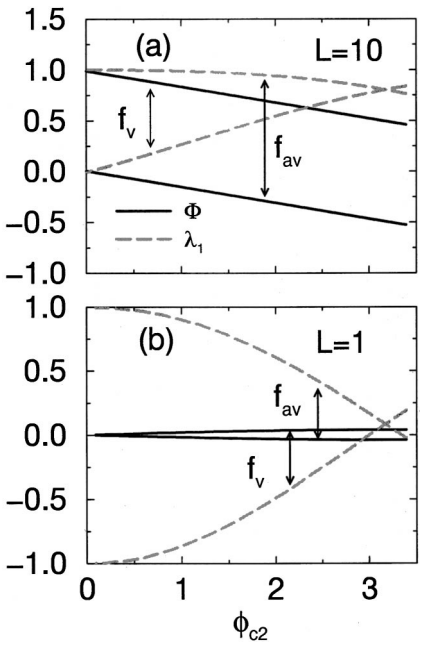

FIG. 5. The evolution of the fractional vortex f_v and antivortex f_{av} as a function of ϕ_{c2}, for two different lengths (a) $L=10$, (b) $L=1$. The stability of theses branches is also denoted by the lowest eigenvalue λ_1 of the linearized eigenvalue problem. Note that the double arrow connects the flux with its stability curve.

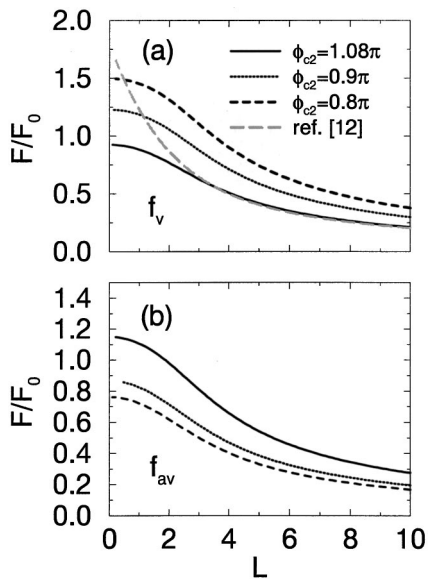

FIG. 6. The ratio of the free energy, F/F_0, as a function of the reduced junction length L, for different values of ϕ_{c2}: (a) f_v, (b) f_{av}.

sides, the unstable vortex solution of the *s*-type junction with $\Phi=1$, as we increase ϕ_{c2}, goes to the f_v of the $d+is$ junction stabilizing itself as seen by the stability analysis from which the lowest eigenvalue is also displayed (light line). If we continue increasing the ϕ_{c2}, it will go to the no-vortex solution of the usual *s*-type junction. The linear dependence of Φ from ϕ_{c2} can also be seen in the analytical result of Ref. 12, for large lengths, where the approximation they made is valid. When we change ϕ_{c1} and keep $\phi_{c2}=0$, from 0 to 2π, the (0,1) branch goes to f_v and then to the unstable (1,2), while the unstable $(-2,-1)$ branch goes to f_{av} and then to the stable (0,1).

The situation is a little bit different for small lengths as can be seen from Fig. 5(b) where $L=1$, $H=0$. Here the stable solution of the *s*-wave junction will be transformed to the f_{av} of the $(d+is)$-wave junction, with the increase of ϕ_{c2}, while the unstable $\Phi=0$ solution of the *s*-wave junction will go to the stable f_v when ϕ_{c2} is equal to 1.08π. Notice that the magnetic flux remains almost constant—almost zero—which can be expected since we are in the short-junction limit where self-currents are neglected.

In Fig. 6 we plot the ratio F/F_0 of the free energy of the state with some spontaneous flux to the state with no flux. This ratio becomes larger than 1 as we decrease the ϕ_{c2}, for the f_v branch, for small lengths. On the other hand, when $F/F_0<1$ the no-flux state is metastable and the final state will be the one with spontaneous flux.

V. CONCLUSIONS

We have studied the static properties of a one-dimensional junction with $d+is$ order parameter symmetry. The magnetic interference pattern is asymmetric, and there exist a ''dip'' near $\Phi=0$ for lengths as long as $10\lambda_J$. The diffraction pattern of a junction can give us information about the pairing symmetry, at least where junctions are formed.

We have followed the evolution of spontaneously formed

vortex and antivortex solutions for different mixing between the s and d components of the order parameter. We have shown that for small lengths the fractional vortex becomes unstable as we decrease the extra phase of the pair transfer integral in the right part of the junction. We conclude that when a mixing state symmetry is realized, the fractional vortex and antivortex solutions evolve differently and this characterizes the $(d+is)$-wave pairing. We expect these findings to hold even if a bulk $d+s$ state evolves continuously as a function of distance from the interface to a $d+is$ one, as long as the there is a well-defined area close to the interface where the time-reversal symmetry is not conserved and the junction is formed.

ACKNOWLEDGMENTS

We are grateful to J. Betouras for his support. N.S. wishes also to thank J. Giapintzakis, G. Psaltakis, and G. Varelogiannis for useful discussions.

[1] D.J. Scalapino, Phys. Rep. **250**, 329 (1995).
[2] D.J. Van Harlingen, Rev. Mod. Phys. **67**, 515 (1995).
[3] D.A. Wollman, D.J. Van Harlingen, J. Giapintzakis, and D.M. Ginsberg, Phys. Rev. Lett. **74**, 797 (1995).
[4] C.C. Tsuei, J.R. Kirtley, C.C Chi, L.S. Yu-Jahnes, A. Gupta, T. Shaw, J.Z. Sun, and M.B. Ketchen, Phys. Rev. Lett. **73**, 593 (1994).
[5] J.R. Kirtley, C.C. Tsuei, and L.S. Yu-Jahnes, Nature (London) **373**, 225 (1995).
[6] J.J. Betouras and R. Joynt, Phys. Rev. B **57**, 11 752 (1998).
[7] J. Ma, C. Quitmann, R.J. Kelley, H. Berger, G. Margaritondo, and M. Onellion, Science **267**, 862 (1995); a theoretical analysis by J. Betouras and R. Joynt, Europhys. Lett. **31**, 119 (1995).
[8] K.A. Kouznetsov, A.G. Sun, B. Chen, A.S Katz, S.R. Bahcall, J. Clarke, R.C. Dynes, D.A. Gajewski, S.H. Han, M.B. Maple, J. Giapintzakis, J.-T. Kim, and D.M. Ginsberg, Phys. Rev. Lett. **79**, 3050 (1997).
[9] K.A. Musaelian, J. Betouras, A.V. Chubukov, and R. Joynt, Phys. Rev. B **53**, 3598 (1996).
[10] Y. Ren, J.H. Xu, and C.S. Ting, Phys. Rev. B **53**, 2249 (1996).
[11] J.R. Kirtley, P. Chaudhari, M.B. Ketchen, N. Khare, S.Y. Lin, and T. Shaw, Phys. Rev. B **51**, 12 057 (1995).
[12] J.-X. Zhu, W. Kim, and C.S. Ting, Phys. Rev. B **58**, 6455 (1998).
[13] D.B. Bailey, M. Sigrist, and R.B. Laughlin, Phys. Rev. B **55**, 15 239 (1997).
[14] L.G. Aslamazov and A.I. Larkin, Pis'ma Zh. Éksp. Teor. Fiz. **9**, 150 (1968) [JETP Lett. **9**, 87 (1969)].
[15] M.B. Walker and J. Luettmer-Strathmann, Phys. Rev. **54**, 588 (1996).
[16] J. Giapintzakis, D.M. Ginsberg, and P.-D. Han, J. Low Temp. Phys. **77**, 155 (1989).
[17] J.H. Xu, J.H. Miller, and C.S. Ting, Phys. Rev. B **51**, 11 958 (1995).
[18] J.R. Kirtley, K.A. Moler, and D.J. Scalapino, Phys. Rev. B **56**, 886 (1997).
[19] C.S. Owen and D.J. Scalapino, Phys. Rev. **164**, 538 (1967).
[20] J.-G. Caputo, N. Flytzanis, Y. Gaididei, N. Stefanakis, and E. Vavalis (unpublished).